

Radio and optical observations of the possible AE Aqr twin, LAMOST J024048.51+195226.9

M. L. Pretorius,^{1*} D. M. Hewitt,^{1,2,3} P. A. Woudt,² R. P. Fender,^{4,2} I. Heywood,^{4,5,6} C. Knigge,⁷ J. C. A. Miller-Jones,⁸ D. A. H. Buckley,¹ H. L. Worters,¹ S. B. Potter,^{1,9} D. R. A. Williams¹⁰

¹South African Astronomical Observatory, PO Box 9, Observatory 7935, South Africa

²Department of Astronomy, University of Cape Town, Private Bag X3, Rondebosch 7701, South Africa

³Anton Pannekoek Institute for Astronomy, University of Amsterdam, Science Park 904, 1098 XH Amsterdam, The Netherlands

⁴Department of Physics, Astrophysics, University of Oxford, Denys Wilkinson Building, Keble Road, Oxford OX1 3RH, UK

⁵Department of Physics and Electronics, Rhodes University, PO Box 94, Makhanda 6140, South Africa

⁶South African Radio Astronomy Observatory, 2 Fir Street, Black River Park, Observatory, Cape Town 7925, South Africa

⁷School of Physics and Astronomy, University of Southampton, Highfield, Southampton, SO17 1BJ, UK

⁸International Centre for Radio Astronomy Research – Curtin University, GPO Box U1987, Perth, WA 6845, Australia

⁹Department of Physics, University of Johannesburg, PO Box 524, Auckland Park 2006, South Africa

¹⁰Jodrell Bank Centre for Astrophysics, School of Physics and Astronomy, The University of Manchester, Manchester, M13 9PL, UK

Accepted XXX. Received YYY; in original form ZZZ

ABSTRACT

Thorstensen (2020) recently argued that the cataclysmic variable (CV) LAMOST J024048.51+195226.9 may be a twin to the unique magnetic propeller system AE Aqr. If this is the case, two predictions are that it should display a short period white dwarf spin modulation, and that it should be a bright radio source. We obtained follow-up optical and radio observations of this CV, in order to see if this holds true. Our optical high-speed photometry does not reveal a white dwarf spin signal, but lacks the sensitivity to detect a modulation similar to the 33-s spin signal seen in AE Aqr. We detect the source in the radio, and measure a radio luminosity similar to that of AE Aqr and close to the highest so far reported for a CV. We also find good evidence for radio variability on a time scale of tens of minutes. Optical polarimetric observations produce no detection of linear or circular polarization. While we are not able to provide compelling evidence, our observations are all consistent with this object being a propeller system.

Key words: accretion, accretion discs – stars: jets – novae, cataclysmic variables – white dwarfs – radio continuum: stars

1 INTRODUCTION

CVs are semi-detached binaries, in which a white dwarf (WD) accretes from a low-mass donor star (see e.g. Warner 1995). In magnetic CVs, the WD has a magnetic field sufficiently strong to alter the accretion flow significantly. These systems are divided into two subtypes, namely polars and intermediate polars (IPs).

Polars are characterized by strong circular and linear polarization, modulated at the orbital period (P_{orb}), indicating WD rotation that is synchronized (or very close to synchronized) with the binary orbit. IPs have highly coherent pulsations, at periods $< P_{orb}$, in their X-ray and/or optical light curves, interpreted as the spin modulation of a WD rotating at a period much shorter than the orbit.

Patterson (1979) discovered very stable optical pulsations at a period of 33.07 s in the nearby CV AE Aqr, leading him to suggest that it is an “oblique rotator” (a system in which the WD spin and magnetic axes are misaligned, and

the accretion flow is magnetically channeled from the inner edge of a truncated accretion disc, onto the WD), the model now used to describe other IPs. de Jager et al. (1994) found that the WD in AE Aqr is spinning down at a high rate (5.6×10^{-14} s/s). AE Aqr was also one of the first CVs to be detected in the radio (Bookbinder & Lamb 1987), and at $\sim 5 \times 10^{16}$ erg s⁻¹ Hz⁻¹ is amongst the most radio luminous CVs (e.g. Bastian, Dulk, & Channugam 1988; Barrett et al. 2017; Coppejans & Knigge 2020). The radio emission is modelled as a superposition of synchrotron sources (Bastian, Dulk, & Channugam 1988).

Besides the 33-s signal, the observed behaviour for which AE Aqr is best known is its spectacular flaring. Many observers have reported large-amplitude aperiodic flaring in optical, X-ray, and radio light curves (on time scales of minutes to tens of minutes), and also in the optical emission lines of this system (e.g. Patterson 1979; Bastian, Dulk, & Channugam 1988; Skidmore et al. 2003; Welsh, Horne, & Gomer 1998; Choi & Dotani 1999, 2006).

The rapid spin-down, with spin-down power greatly exceeding the radiated power, the lack of evidence for a

* E-mail: retha@sao.ac.za (MLP)

disc, and the spectacular flares seen in AE Aqr are explained by a “magnetic propeller” where the rapidly rotating, strongly magnetic WD expels most of the infalling gas, preventing it from accreting (Eracleous & Horne 1996; Wynn, King, & Horne 1997). AE Aqr remains the only CV that is modelled as a magnetic propeller, and up until recently, had the shortest known WD spin period¹.

The recently discovered LAMOST J024048.51+195226.9, also catalogued as CRTS J024048.5+195227, (hereafter J0240) may be another example of a magnetic propeller. Thorstensen (2020) points out several optical properties reminiscent of AE Aqr, including large-amplitude flares on time scales down to ~ 1 minute, weak or absent $\text{He II } \lambda 4686$ emission (usually very strong in magnetic CVs, but not in AE Aqr), and emission lines that show irregular variations, with radial velocities that do not seem to trace the orbit. The system has an orbital period of 7.3 hours (Drake et al. 2014; Thorstensen 2020; Littlefield & Garnavich 2020).

If J0240 really is another propeller system, an observational signature would be a rapid WD spin modulation in optical and/or X-ray light curves (the light curves of Thorstensen (2020) had only 23 and 30 s cadence). One would also expect it to show bright radio emission, by analogy with AE Aqr. Here we present the first radio detection of J0240, as well as optical high-speed photometry and photo-polarimetry. Our observations are described in Section 2. The results are presented and discussed in Section 3. Finally, Section 4 summarizes our work.

2 OBSERVATIONS

We obtained radio and optical data of J0240 in the second half of 2020, using the MeerKAT radio interferometer, the South African Astronomical Observatory (SAAO) 1-m optical telescope, Lesedi, and the SAAO 74-inch telescope. Table 1 gives a log of the observations.

2.1 MeerKAT radio interferometer

A roughly 2 hour observation was taken with MeerKAT on 12 Aug 2020, as part of the ThunderKAT survey (The Hunt for Dynamic and Explosive Radio Transients using MeerKAT; Fender et al. 2017). The observation was done in the L-band (centered at 1284 MHz, with a bandwidth of 856 MHz covered by 4096 channels), using 59 of the 64 antennas. It started and ended with scans of the primary calibrator (J0408-6545), and alternated between the secondary calibrator (J0238+1636) and target for the rest of the observation. Visibilities were recorded every 2 seconds, and the 6 target scans were each approximately 15 minutes in length.

The data were calibrated and imaged using the OxKAT² pipeline (Heywood 2020). This implements standard CASA (e.g. McMullin et al. 2007) routines, as well as the SARAO

tricolour flagger³, and the imaging packages DDFacet (Tasse et al. 2018) and WSCLEAN (Offringa et al. 2014). We found that second generation calibration (direction independent self-calibration) does not significantly improve the image quality in the region near the target, and therefore report results obtained from applying only first generation calibration. Noise and flux density measurements were performed with PyBDSF (Mohan & Rafferty 2015).

2.2 Optical photometry with the Lesedi 1-m telescope

We observed J0240 on three consecutive nights in September 2020 with the new 1-m optical telescope, Lesedi, at the SAAO site in Sutherland. We performed high-speed photometry in white light (i.e. filterless photometry), using the imager SHOC (Gulbis et al. 2011; Coppejans et al. 2013). The integration time was 5 s on all nights, and since this is a frame-transfer CCD, there was no dead-time between integrations. Only quite short (< 3 hours) observations were possible at the northern declination of J0240, and this early in the season.

We used the TEA-Phot⁴ code (Bowman & Holdsworth 2019) to extract the photometry. Since no filter was used, it is not possible to precisely place these data on a standard photometric system. However, by comparing the instrumental magnitudes of several stars in the field with catalogued *B*- and *R*-band measurements, we are able to perform a very rough calibration (to within 0.1 mag), and verify that J0240 was at about the same brightness as during the observations of Thorstensen (2020), just above 17th magnitude for most of the time⁵.

2.3 Optical all-Stokes Polarimetry with the 74-inch telescope

Photo-polarimetry of J0240 was obtained on a single night in November 2020, over a period of ~ 1 hour, using the SAAO 74-inch telescope with the High-speed Photo-Polarimeter (HIPPO; Potter et al. 2010). This instrument performs time-resolved, simultaneous all-Stokes observations. No filter was used, implying a very broad bandpass (roughly 3500 to 9000 Å). The polarimetric data were reduced as described in Potter et al. (2010).

3 RESULTS AND DISCUSSION

3.1 The radio data

The radio map, with contours overlaid, of a small area at the center of the MeerKAT field is shown in Fig. 1. We detect a bright radio point source coincident with the optical position of J0240, and assume it is the CV. The integrated radio flux density of J0240 is 0.60 ± 0.02 mJy, and the RMS noise measured nearby is $9.0 \mu\text{Jy beam}^{-1}$.

Splitting the 865 MHz bandwidth into 8 frequency subbands, we measure an in-band spectral index of $\alpha = -0.6 \pm 0.2$ (where $S_\nu \propto \nu^\alpha$). Note, however, that there are still bandpass calibration uncertainties for MeerKAT, and also that the

¹ In the last few months, very short WD spin periods were identified in two CVs, CTCVJ2056-3014 and V1460 Her (29.6 and 38.6 s, respectively). These systems however both have at least partial discs and are accretion powered; i.e. apart from harbouring rapidly spinning WDs, they are similar to normal IPs, rather than to AE Aqr (Lopes de Oliveira et al. 2020; Ashley et al. 2020).

² Available from <https://github.com/IanHeywood/oxkat/>

³ <https://github.com/ska-sa/tricolour/>

⁴ <https://bitbucket.org/DominicBowman/tea-phot/src/master/>

⁵ Long-term CRTS, ASAS-SN, and ATLAS photometry also show no evidence of outbursts or low states in J0240.

Table 1. Log of the observations of J0240. The MeerKAT radio observations used J0408-6545 as primary calibrator and J0238+1636 as secondary calibrator. For the Lesedi photometry, the integration time (and time resolution) was 5 s on all nights.

Start Date and Time (UTC)	Total time on target (hours)
MeerKAT	
2020 Aug 12 00:18:49.7	1.501
Lesedi + SHOC	
2020 Sep 8 00:19:46.0	2.499
2020 Sep 9 00:56:22.0	2.653
2020 Sep 10 00:07:45.0	2.012
74-inch + HIPPO	
2020 Nov 12 22:27:41.0	1.117

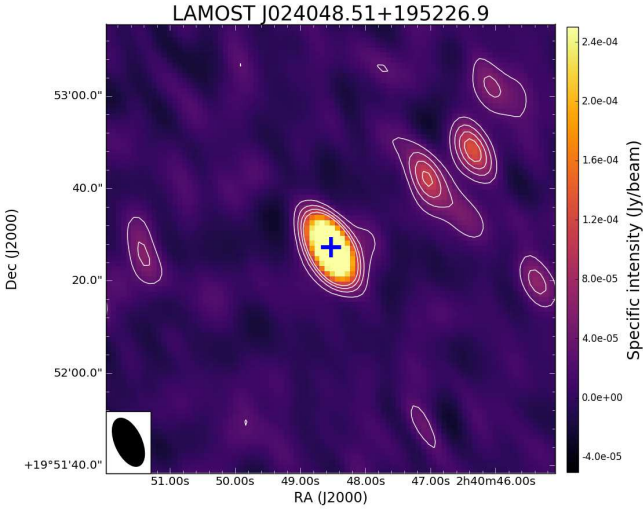


Figure 1. A $100'' \times 100''$ area of the MeerKAT radio map of the J0240 field, with north up and east to the left. The RMS noise in the vicinity of the point source at the center is $9.0 \mu\text{Jy beam}^{-1}$, and contours are at 3, 6, 9, and $12 \times$ the RMS value. The blue cross marks the optical position of J0240, as measured by *Gaia* (the size of this symbol does not denote anything). The inset in the bottom left-hand corner shows the beam shape and size ($11.42'' \times 6.11''$ with a position angle of 29.2°).

source is variable (see below). In the case of AE Aqr, the time averaged spectral index is positive (Abada-Simon et al. 1993; Dubus et al. 2007), but it varies rapidly, as may be expected from a changing optical depth in synchrotron emitting blobs (Bastian, Dulk, & Channugam 1988).

At the *Gaia* Early Data Release 3 (Gaia Collaboration et al. 2016, 2020) distance of 620 ± 30 pc, J0240 has a specific radio luminosity of $2.7 \pm 0.3 \times 10^{17} \text{ erg s}^{-1} \text{ Hz}^{-1}$, placing it amongst the most radio-luminous CVs. Fig. 2 shows radio luminosity as a function of orbital period for CVs belonging to different classes (see Coppejans & Knigge 2020 for an earlier version of this plot). Besides J0240, this includes all CVs with known distances and recent, sensitive radio observations between ~ 1 and 12 GHz. In addition, we include the WD pulsar, AR Sco (Marsh et al. 2016; Marcote et al. 2017). The highest point in this plot (belonging to the IP V1323 Her) is at slightly lower luminosity than shown in Coppejans & Knigge (2020), because the distance was revised down (from 2240 to 1950 pc) in the *Gaia* EDR3.

While J0240, AE Aqr, and the two normal IPs shown in Fig. 2 are all similarly radio-luminous, IPs are detected at radio wavelengths at a rate of $\lesssim 10\%$. Barrett et al. (2017) obtained sensitive VLA observations of more than 40 IPs and candidate IPs, including several well-studied systems at smaller distances than J0240, and (besides AE Aqr) detected only two. These two IPs, V1323 Her and Cas 1 (also known as RX J0153.3+7446) are both at large distances ($\gtrsim 1.5$ kpc), and have only low S/N detections in only a small subset of the VLA observations (Barrett et al. 2017).

In order to look for radio variability, we split the observations into six 15 minute time bins, corresponding to the on-target scans, and imaged each of these epochs separately. Fig. 3 shows the resulting radio light curves. The bottom panel is the integrated radio flux density as a function of time, showing that J0240 varies by $> 5\sigma$, on a timescale of tens of minutes. The top panel of Fig. 3 shows each time bin further split into two equal frequency bins.

If we assume that the radio emission is due to synchrotron radiation, and that we caught the end of a radio flare that evolved from optically thick to optically thin because of a decreasing optical depth to synchrotron self absorption, we can estimate a minimum energy following Fender & Bright (2019). Assuming further that the flare peaked at 0.8 mJy (at 1.5 GHz), then, for an integrated radio luminosity of $2.2 \times 10^{31} \text{ erg s}^{-1}$, the minimum energy is $1.5 \times 10^{35} \text{ erg}$. This value corresponds to an emitting region size of $1.0 \times 10^{12} \text{ cm}$ and a plasma magnetic field of 0.53 G. This energy is higher than the minimum energy found for a radio flare from SS Cyg by Fender et al. (2019), but the uncertainty on our estimate is at least an order of magnitude.

3.2 The optical high-speed photometry

The optical light curves of J0240 are displayed in Fig. 4. These are all differential light curves, implying that colour differences between J0240 and comparison stars were ignored in correcting the photometry for atmospheric extinction. The system displays the rapid flickering typically seen in CVs (the observational signature of mass transfer), but these short runs show very little of the flaring reported by Thorstensen (2020). The photometry is also of fairly low quality, since it was obtained mainly in conditions of poor seeing.

Our Nyquist frequency of 0.1 Hz should be sufficiently high to allow a detection of the WD spin signal. A higher spin frequency would imply a WD above $1 M_\odot$ (see e.g. Otoniel et al. 2020). While this is of course possible, there is nothing to indicate that the WD in J0240 is more massive than the $\simeq 0.8 M_\odot$ more commonly measured for WDs in CVs (a mass that would imply a break-up spin period closer to 20 s).

Fig. 5 shows discrete Fourier transforms of our optical light curves. We detect no coherent signals. It would, however, not be at all surprising if this system is in future found to have an optical modulation similar to the 33-s signal in AE Aqr. In his optical data of AE Aqr, Patterson (1979) observed an amplitude exceeding 1% (corresponding to $2.5 \log(101/100) \simeq 0.01 \text{ mag}$) at times during flares, but the average amplitude was only 0.2 to 0.3%. Beskrovnyaya, Ikhsanov, & Bruch (1995) also reported no detection in photometry spanning 4 weeks, implying a conservative upper limit amplitude of $< 0.005 \text{ mag}$. Fig. 6 zooms in on the high frequency end of the Fourier transform of the combined J0240 light curve (this of course has

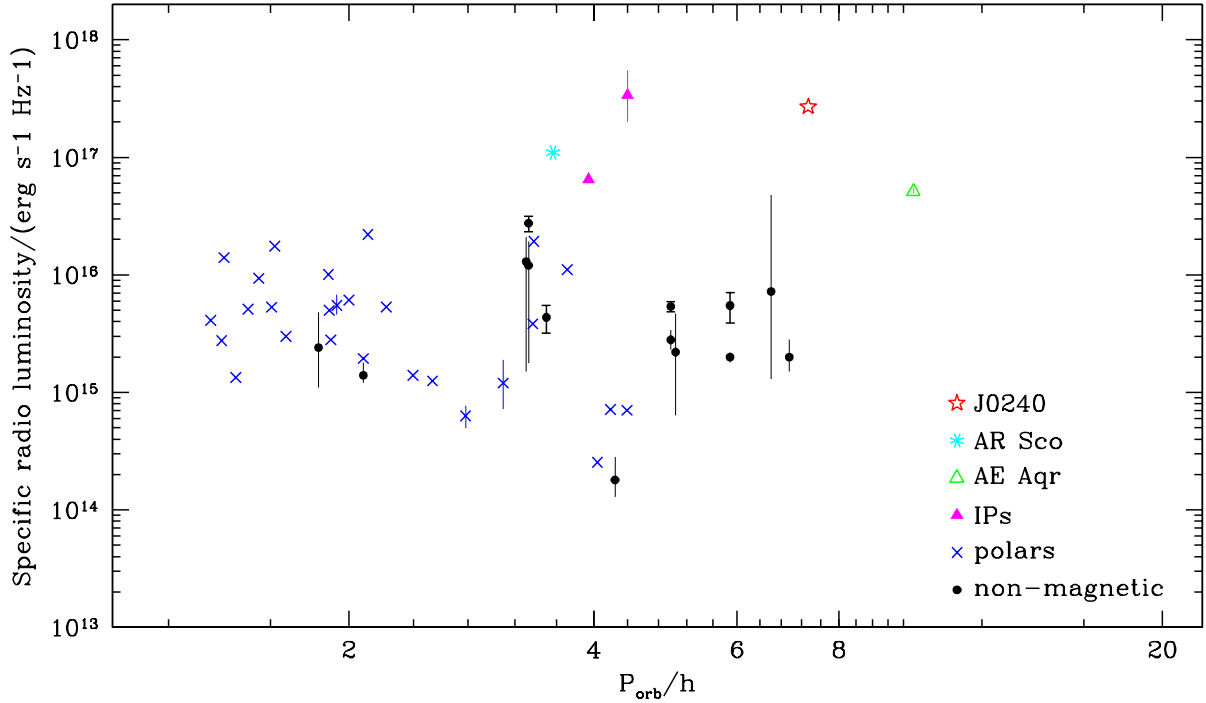


Figure 2. Radio luminosities as a function of orbital period for 42 CVs and the WD pulsar AR Sco. The CV classes are distinguished by different symbols. Some of these systems have been observed at a range of radio flux densities, which we indicate with the fine vertical bars. The error bars for J0240 are not shown, but are smaller than the symbol size. Points with error bars are the L-band observations from [Hewitt et al. \(2020\)](#); other data are at higher frequencies, mainly C- and X-band, and are from [Coppejans et al. \(2016, 2015\)](#); [Körding et al. \(2008\)](#); [Miller-Jones et al. \(2011\)](#); [Russell et al. \(2016\)](#); [Marsh et al. \(2016\)](#); [Marcote et al. \(2017\)](#); [Barrett et al. \(2017, 2020\)](#).

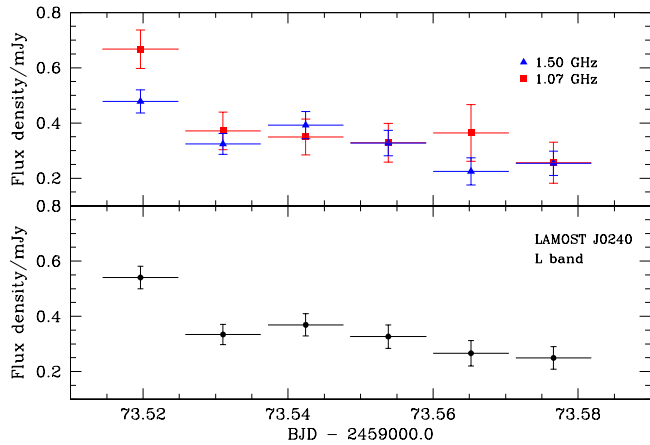


Figure 3. The radio light curve of J0240, constructed from the data shown in Fig. 1. Each time bin is close to 15 minutes. The bottom panel shows the full L-band data, while in the top panel, this was split into 2 frequency sub-bands, centered on 1.07 GHz and 1.50 GHz.

lower white noise than the Fourier transforms of individual light curves, but actually also has less sensitivity to a signal that is present for only a short while). This shows that while there is no persistently present signal at the 1% level in these data, a 0.2 to 0.3% signal would be well below the noise level. Our photometry therefore cannot rule out a rapidly spinning WD giving rise to a modulation very similar to the one observed in AE Aqr.

For the interpretation of J0240 as a magnetic propeller, it re-

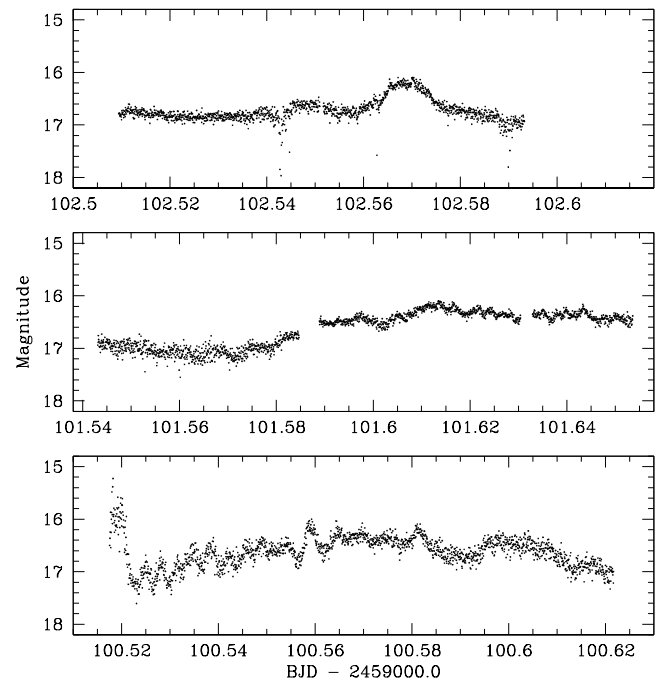


Figure 4. The unfiltered optical light curves of J0240, at 5-s time resolution, on 3 consecutive nights. Seeing conditions were especially poor on the third night (top panel). The very low points in that light curve are measured in frames with very bad image quality; these spurious points were removed before the Fourier transforms were calculated.

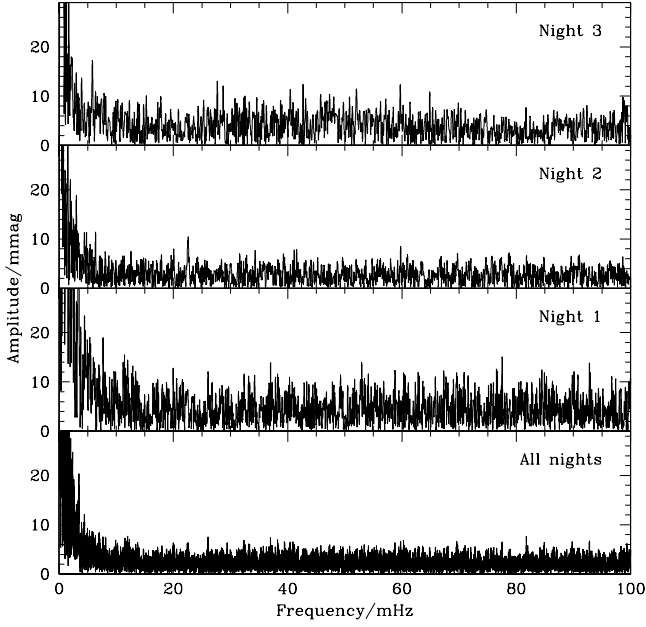


Figure 5. Fourier transforms of the optical light curves of J0240. In the top 3 panels, Fourier transforms of the light curves taken on each of the 3 nights are shown individually, while the Fourier transform in the bottom panel is of all data combined.

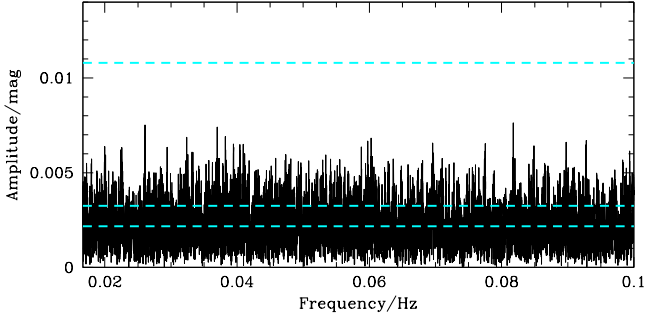


Figure 6. The Fourier transform of all 3 nights of photometry combined, showing only the frequency range corresponding to periods between 60 and 10 s. Dashed horizontal lines indicate amplitudes of 0.2, 0.3, and 1%.

mains key to demonstrate that this system contains a rapidly spinning WD. Longer optical light curves may show this. Alternatively, X-ray or UV timing would be worth obtaining (J0240 has not yet been detected at X-ray or UV frequencies). The 33-s signal of AE Aqr has an amplitude $>20\%$ in X-rays (Patterson et al. 1980).

3.3 The optical polarimetry

There was no significant detection of polarization. Our measurement of time-averaged circular polarization is $0.10\% \pm 0.07\%$, consistent with a value of zero. For the time-averaged linear polarization, we find $1.3\% \pm 0.1\%$, consistent with an interstellar (or instrumental) origin.

Polarimetric observations of AE Aqr have yielded possible, marginal detections of circular polarization, but at levels of \lesssim

0.1% (e.g. Cropper 1986; Beskrovnaya et al. 1996; Butters et al. 2009).

4 SUMMARY

We have presented radio L-band imaging, and optical high-speed photometry and photo-polarimetry of the recently discovered CV, J0240. Our aim was to examine the similarity of J0240 to the magnetic propeller system, AE Aqr. The high radio luminosity supports the suggestion that this system may be an AE Aqr-like object. However, the most important question, which we are unable to answer, is whether it contains a rapidly spinning WD. The main results of this study are listed below.

- (i) J0240 is detected as a bright radio source. We measure a 1.284 GHz flux density of 0.60 ± 0.02 mJy, and an in-band spectral index of -0.6 ± 0.2 .
- (ii) The radio luminosity of $2.7 \pm 0.3 \times 10^{17}$ erg s $^{-1}$ Hz $^{-1}$ is the second highest yet reported for a CV.
- (iii) The system varies in the radio on a time scale of 10s of minutes.
- (iv) We fail to detect any coherent signal that can be attributed to a rapidly spinning WD in our 3 nights of optical high-speed photometric observations.
- (v) Although we are able to search for signals with periods down to 10 s, the sensitivity of our high-speed photometry to low amplitude signals is not sufficient to rule out a WD spin modulation similar to the 33-s signal seen in AE Aqr.
- (vi) There was no detection of linear or circular polarization in the optical.

ACKNOWLEDGEMENTS

MLP acknowledges financial support from the National Research Foundation (NRF) and the Newton Fund. PAW acknowledges financial support from the University of Cape Town and the NRF. We thank John Thorstensen for helpful discussions of the system that this work focusses on. Sara Motta kindly looked at the archived *Swift* data of this object, to confirm that there is no X-ray detection. The MeerKAT telescope is operated by the South African Radio Astronomy Observatory (SARAO), which is a facility of the NRF, an agency of the Department of Science and Innovation. We thank the SARAO staff involved in obtaining the MeerKAT observations. We made use of the computing facilities of the Inter-University Institute for Data Intensive Astronomy (IDIA) in this research.

DATA AVAILABILITY

The data presented in this article are subject to the standard data access policies of the South African Radio Astronomy Observatory and the South African Astronomical Observatory.

REFERENCES

- Abada-Simon M., Lecacheux A., Bastian T. S., Bookbinder J. A., Dulk G. A., 1993, *ApJ*, 406, 692. doi:10.1086/172479

- Ashley R. P., Marsh T. R., Breedt E., Gänsicke B. T., Pala A. F., Toloza O., Chote P., et al., 2020, *MNRAS*, 499, 149
- Barrett P. E., Dieck C., Beasley A. J., Singh K. P., Mason P. A., 2017, *AJ*, 154, 252
- Barrett P., Dieck C., Beasley A. J., Mason P. A., Singh K. P., 2020, *AdSpR*, 66, 1226
- Bastian T. S., Dulk G. A., Chanmugam G., 1988, *ApJ*, 324, 431
- Beskrovnaya N., Ikhsanov N., Bruch A., 1995, *ASSL*, 368
- Beskrovnaya N. G., Ikhsanov N. R., Bruch A., Shakhovskoy N. M., 1996, *A&A*, 307, 840
- Bookbinder J. A., Lamb D. Q., 1987, *ApJL*, 323, L131
- Bowman D. M., Holdsworth D. L., 2019, *A&A*, 629, A21
- Butters O. W., Katajainen S., Norton A. J., Lehto H. J., Piirola V., 2009, *A&A*, 496, 891
- Choi C. S., Dotani T., 1999, *AN*, 320, 348
- Choi C.-S., Dotani T., 2006, *ApJ*, 646, 1149
- Coppejans D. L., Knigge C., 2020, *NewAR*, 89, 101540
- Coppejans D. L., K rding E. G., Miller-Jones J. C. A., Rupen M. P., Sivakoff G. R., Knigge C., Groot P. J., et al., 2016, *MNRAS*, 463, 2229
- Coppejans D. L., K rding E. G., Miller-Jones J. C. A., Rupen M. P., Knigge C., Sivakoff G. R., Groot P. J., 2015, *MNRAS*, 451, 3801
- Coppejans R., Gulbis A. A. S., Kotze M. M., Coppejans D. L., Worters H. L., Woudt P. A., Whittal H., et al., 2013, *PASP*, 125, 976
- Cropper M., 1986, *MNRAS*, 222, 225
- de Jager O. C., Meintjes P. J., O'Donoghue D., Robinson E. L., 1994, *MNRAS*, 267, 577
- Drake A. J., Graham M. J., Djorgovski S. G., Catelan M., Mahabal A. A., Torrealba G., Garc a- lvarez D., et al., 2014, *ApJS*, 213, 9
- Dubus G., Taam R. E., Hull C., Watson D. M., Mauerhan J. C., 2007, *ApJ*, 663, 516
- Eracleous M., Horne K., 1996, *ApJ*, 471, 427
- Fender R., Bright J., 2019, *MNRAS*, 489, 4836
- Fender R., et al., 2017, eprint arXiv:1711.04132
- Fender R., Bright J., Mooley K., Miller-Jones J., 2019, *MNRAS*, 490, L76
- Gulbis A. A. S., O'Donoghue D., Fourie P., Rust M., Sass C., Stofels J., 2011, *epsc.conf*, 2011, 1173
- Heywood I., 2020, *ascl.soft. ascl:2009.003*
- Hewitt D. M., Pretorius M. L., Woudt P. A., Tremou E., Miller-Jones J. C. A., Knigge C., Castro Segura N., et al., 2020, *MNRAS*, 496, 2542
- K rding E., Rupen M., Knigge C., Fender R., Dhawan V., Templeton M., Muxlow T., 2008, *Sci*, 320, 1318
- Gaia Collaboration, Prusti T., de Bruijne J. H. J., Brown A. G. A., Vallenari A., Babusiaux C., Bailer-Jones C. A. L., et al., 2016, *A&A*, 595, A1
- Gaia Collaboration, Brown A. G. A., Vallenari A., Prusti T., de Bruijne J. H. J., Babusiaux C., Biermann M., 2020, *arXiv*, arXiv:2012.01533
- Littlefield C., Garnavich P., 2020, *RNAAS*, 4, 171
- Lopes de Oliveira R., Bruch A., Rodrigues C. V., Oliveira A. S., Mukai K., 2020, *ApJL*, 898, L40
- Marcote B., Marsh T. R., Stanway E. R., Paragi Z., Blanchard J. M., 2017, *A&A*, 601, L7
- Marsh T. R., G nsicke B. T., H mmerich S., Hamsch F.-J., Bernhard K., Lloyd C., Breedt E., et al., 2016, *Natur*, 537, 374
- McMullin J. P., Waters B., Schiebel D., Young W., Golap K., 2007, *ASPC*, 376, 127
- Miller-Jones J. C. A., Sivakoff G. R., Altamirano D., K rding E. G., Krimm H. A., Maitra D., Remillard R. A., et al., 2011, *IAUS*, 275, 224
- Mohan N., Rafferty D., 2015, *ascl.soft. ascl:1502.007*
- Offringa A. R., McKinley B., Hurley-Walker N., Briggs F. H., Wayth R. B., Kaplan D. L., Bell M. E., et al., 2014, *MNRAS*, 444, 606
- Otoniel E., Coelho J. G., Malheiro M., Weber F., 2020, *arXiv*, arXiv:2010.12441
- Patterson J., 1979, *ApJ*, 234, 978
- Patterson J., Branch D., Chincarini G., Robinson E. L., 1980, *ApJL*, 240, L133
- Potter S. B., Buckley D. A. H., O'Donoghue D., Romero-Colmenero E., O'Connor J., Fourie P., Evans G., et al., 2010, *MNRAS*, 402, 1161
- Skidmore W., O'Brien K., Horne K., Gomer R., Oke J. B., Pearson K. J., 2003, *MNRAS*, 338, 1057
- Tasse C., Hugo B., Mirmont M., Smirnov O., Atemkeng M., Bester L., Hardcastle M. J., et al., 2018, *A&A*, 611, A87
- Thorstensen J. R., 2020, *AJ*, 160, 151
- Russell T. D., Miller-Jones J. C. A., Sivakoff G. R., Altamirano D., O'Brien T. J., Page K. L., Templeton M. R., et al., 2016, *MNRAS*, 460, 3720
- Warner B., 1995, *Cataclysmic Variable Stars*. Cambridge Univ. Press, Cambridge
- Welsh W. F., Horne K., Gomer R., 1998, *MNRAS*, 298, 285
- Wynn G. A., King A. R., Horne K., 1997, *MNRAS*, 286, 436. doi:10.1093/mnras/286.2.436

This paper has been typeset from a \LaTeX file prepared by the author.